Developmental Increase in Vesicular Glutamate Content Does Not Cause Saturation of AMPA Receptors at the Calyx of Held Synapse

Takayuki Yamashita, Taro Ishikawa, and Tomoyuki Takahashi
Department of Neurophysiology, University of Tokyo Graduate School of Medicine, Tokyo 113-0033, Japan

Whether a quantal packet of transmitter saturates postsynaptic receptors is a fundamental question in central synaptic transmission. However, this question remains open with regard to saturation at mature synapses. The calyx of Held, a giant glutamatergic synapse in the auditory brainstem, becomes functionally mature during the fourth postnatal week in rats. During postnatal development, the mean amplitude of miniature (i.e., quantal) EPSCs (mEPSCs) becomes significantly larger. Experiments using the rapidly dissociating glutamate receptor antagonist kynurenate suggested that vesicular glutamate content increases with development. To test whether AMPA receptors are saturated by a packet of transmitter, we infused a high concentration of L-glutamate into mature calyceal terminals. This caused a marked increase in the mean amplitude of mEPSCs. We conclude that a single packet of transmitter glutamate does not saturate postsynaptic AMPA receptors even at the mature calyx of Held synapse with increased vesicular transmitter content.

Key words: **quantal EPSCs; calyx of Held; AMPA receptor; postnatal development; receptor saturation; vesicular transmitter content**

Introduction

Whereas saturation of postsynaptic glutamate receptors by quantal transmitter has been a long-standing hypothesis (Jack et al., 1981; Larkman et al., 1991; Clements et al., 1992; Jonas et al., 1993; Tang et al., 1994; Tong and Jahr, 1994; for review, see Frerking and Wilson, 1996), recent studies at putative single-site synapses suggest that a single packet of transmitter does not saturate postsynaptic AMPA receptors (Silver et al., 1996; Liu et al., 1999) or NMDA receptors (Mainen et al., 1999; Umemiya et al., 1999; McAllister and Stevens, 2000). At the calyx of Held synapse, it has been demonstrated that a high concentration of L-glutamate directly loaded into the giant nerve terminal significantly increases the mean amplitudes of quantal AMPA-EPSCs and quantal NMDA-EPSCs, indicating that a single vesicular transmitter does not saturate postsynaptic glutamate receptors (Ishikawa et al., 2002). However, synapses used for these studies are either in culture or in slices of immature animals, where transmitter packaging might still be under development. At the *Xenopus* neuromuscular junction in culture, synaptic vesicles are incompletely filled with the transmitter acetylcholine at the immature stage (Evers et al., 1989; Song et al., 1997). At the cerebellar mossy fiber–granule cell synapse, the variation in quantal size is large at immature synapses but significantly decreases as animals mature (Wall and Usowicz, 1998). These observations raise the possibility that quantal transmitter may saturate postsynaptic glutamate receptors as animals mature. We examined this possibility using simultaneous presynaptic and postsynaptic recordings at the mature calyx of Held synapse.

Received Jan. 2, 2003; revised Jan. 31, 2003; accepted Feb. 4, 2003.

This study was supported by a grant-in-aid for Specially Promoted Research from the Ministry of Education, Culture, Sports, Science and Technology to T.T. We thank Yoshinori Sahara and Tetsuhiro Tsujimoto for helpful comments on this manuscript.

Correspondence should be addressed to Dr. Tomoyuki Takahashi, Department of Neurophysiology, University of Tokyo Graduate School of Medicine, 7-3-1 Hongo, Bunkyo-ku, Tokyo 113-0033, Japan. E-mail: ttakahastky@umin.ac.jp.

 0270-6474/03/233633-06$15.00/0

Materials and Methods

Preparation and solutions. All experiments were performed in accordance with the guidelines of the Physiological Society of Japan. Transverse brainstem slices (125–300 μm thick) containing the medial nucleus of the trapezoid body (MNTB) were prepared from 6- to 29-d-old [postnatal day 6 (P6)–P29] Wistar rats killed by decapitation under halothane anesthesia (Forsythe and Barnes-Davies, 1993). Slices were incubated for 1 hr at 36–37°C and maintained thereafter at room temperature (22–28°C). The extracellular artificial CSF (aCSF) for perfusion contained (in mM): 125 NaCl, 2.5 KCl, 26 $NaHCO_3$, 1.25 NaH_2PO_4, 2 $CaCl_2$, 1 $MgCl_2$, 10 glucose, 3 myoinositol, 2 sodium pyruvate, and 0.5 ascorbic acid, pH 7.4 when bubbled with 95% O_2 and 5% CO_2, 310–320 mOsm. The aCSF routinely contained bicuculline methiodide (10 μM; Sigma, St. Louis, MO) and strychnine hydrochloride (0.5 μM; Sigma) to block inhibitory synaptic responses. Principal neurons in the MNTB and the presynaptic terminal, the calyx of Held, were visually identified with a 60× water immersion objective (Olympus Optical, Tokyo, Japan) attached to an upright microscope (BX50WI; Olympus Optical; or Axioskop 2; Zeiss, Oberkochen, Germany). Patch pipettes for postsynaptic recordings were filled with (in mM): 110 CsF, 30 CsCl, 10 HEPES, 5 EGTA, and 1 $MgCl_2$, pH adjusted to 7.3–7.4 with CsOH, 290–295 mOsm. *N*-(2,6-Diethylphenylcarbamoylmethyl)-triethyl-ammonium chloride (5 mM; Alomone Labs, Jerusalem, Israel) was routinely included in the postsynaptic pipette solution to suppress action potential generation. Tetrodotoxin (TTX; 0.5–1 μM; Wako, Osaka, Japan) was added to the aCSF for recording miniature EPSCs (mEPSCs). Presynaptic pipette solutions contained (in mM): 105 potassium gluconate, 30 KCl, 10 HEPES, 0.5 EGTA, 12 phosphocreatine (Na salt), 3 ATP (Mg salt), 0.5 GTP (Na salt), and 1 $MgCl_2$, pH 7.3–7.4, adjusted with KOH, 290–300 mOsm. The L-glutamate solution for presynaptic infusion was prepared by replacing potassium gluconate in the pipette solution by L-glutamate to maintain constant osmolarity. Infusion of the L-glutamate solution into calyces was made using a plastic tube installed in a presynaptic patch pipette as reported previously (Hori et al., 1999; Ishikawa et al., 2002). Briefly, a tube with an outer tip diameter of 50–70 μm was fabricated from an

Eppendorf yellow tip and back-filled with the L-glutamate solution. The tube was inserted into a patch pipette to 500–700 μm behind the tip of the pipette. The L-glutamate solution in the tube was ejected with positive pressure applied manually through a syringe.

Recording. Whole-cell recordings were made from the MNTB principal neurons using a patch-clamp amplifier (Axopatch 200B or Multiclamp 700A; Axon Instruments, Foster City, CA). The postsynaptic pipette was pulled for the resistance of 2–3 MΩ and had access resistance of 4–8 MΩ. The presynaptic pipette was pulled for the resistance of 6–10 MΩ and had access resistance of 18–30 MΩ. No compensation was made for the access resistance. The postsynaptic cells were voltage-clamped at a holding potential of −70 mV. Routinely, before recording mEPSCs, EPSCs were evoked at 0.04–0.1 Hz by extracellular stimulation with a bipolar tungsten electrode positioned halfway between the midline and the MNTB (Forsythe and Barnes-Davies, 1993) to ensure that the cells receive calyceal inputs. EPSCs derived from the calyx of Held synapse were identified as those evoked in an all-or-none manner for graded stimulus intensity and having amplitudes >1 nA at −70 mV (Forsythe and Barnes-Davies, 1993). In simultaneous presynaptic and postsynaptic recordings, EPSCs were evoked by presynaptic action potentials elicited by a 1 msec depolarizing pulse (Takahashi et al., 1996), and spontaneous mEPSCs were recorded in the presence of TTX with presynaptic terminals voltage-clamped at −70 mV.

Data analysis. Records were low-pass filtered at 5 kHz and stored on digital audio tapes (sampling rate, 48 kHz). Data were digitized at 50 kHz by a Digidata 1320A analog–digital converter with pClamp8 software (Axon Instruments, Foster City, CA) and analyzed off-line using Axograph (Axon Instruments). Spontaneous and mEPSCs having an amplitude more than three times the baseline noise level (SD, 3–4 pA) were detected using a sliding template method implemented in Axograph. The templates were made by averaging 40–50 mEPSCs. Overlapped mEPSCs were excluded from analyses by visual inspection. The decay time of averaged mEPSCs was fitted to double exponential functions, and its weighted mean (τ_m) was calculated from individual time constants (τ_1, τ_2) and their relative amplitude (a_1, a_2) as follows: $\tau_m = a_1\tau_1 + a_2\tau_2$. For the nonstationary fluctuation analysis, the difference between individual mEPSCs and peak-scaled averaged mEPSCs at their decay phases was calculated, and the ensemble variance was plotted against the current amplitude (Traynelis et al., 1993). Assuming binomial statistics of the channel opening, the σ^2–I relationship is expected to be a parabolic function [i.e., it can be fitted by the following equation: $\sigma^2 = iI - (I^2/N) + \sigma^2_B$, where I represents the mean current, σ^2 represents the peak-scaled variance, N represents the average number of channels open at the peak, i represents the single-channel current amplitude, and σ^2_B represents the background noise variance]. Although plots of experimental data tended to deviate from symmetrical parabola, the initial slope of the σ^2–I relationship provides a reliable estimate for the weighted single-channel current (Silver et al., 1996). All values are given as mean ± SEM. Statistical analysis for two samples was made using Student's t test unless otherwise noted. For multiple comparisons, the Sheffe test was used unless otherwise noted. A value of $p < 0.05$ was taken as the level of significance.

Results

Developmental changes in the quantal EPSCs

Spontaneous mEPSCs mediated by AMPA receptors (Futai et al., 2001) were recorded from the MNTB principal neurons in the presence of TTX. These mEPSCs likely derived from the calyx of Held terminal, because their amplitude distribution is indistinguishable from those evoked by direct steady depolarizations of the nerve terminal in the presence of TTX (Sahara and Takahashi, 2001). The mean amplitude of mEPSCs remained similar from P6–P7 (40.3 ± 3.0 pA; $n = 10$ cells) to P13–P14 (47.1 ± 1.9 pA; $n = 10$) (Figs. 1, 2*A*), as reported previously (Chuhma and Ohmori, 1998; Taschenberger and von Gersdorff, 2000; Iwasaki and Takahashi, 2001), but significantly increased thereafter to P20–P21 (61.7 ± 3.7 pA; $n = 10$) on average by 31% (between P13–P14 and P20–P21; $p < 0.02$; Sheffe test). It then reached a plateau with no additional increase to P28–P29 (59.1 ± 2.7 pA; $n = 10$). The mean quantal frequency also increased by 4.3-fold from P6–P7 (0.26 ± 0.02 Hz) to P20–P21 (1.1 ± 0.2 Hz; $p < 0.04$) and reached a steady level (1.3 ± 0.3 Hz) at P28–P29 (Fig. 2*B*).

In addition to the mean quantal amplitude, the kinetics of mEPSCs changed with postnatal development. The rise time (10–90%) of mEPSCs became significantly shorter from P6–P7 (0.30 ± 0.02 msec) to P13–P14 (0.15 ± 0.01 msec; $p < 0.01$; Sheffe test) (Fig. 2*C*) as reported previously (Taschenberger and von Gersdorff, 2000; Futai et al., 2001) and reached a minimal level thereafter (0.13 ± 0.01 msec in P20–P21 and 0.13 ± 0.004 msec in P28–P29) (Futai et al., 2001). Such a phenomenon is not observed for GABAergic (P4–P40) (Okada et al., 2000) or glycinergic (P0–P18) (Singer et al., 1998) miniature synaptic currents where the rise time remains constant throughout development. The weighted mean time constant of mEPSCs (see Materials and Methods) decreased from P6–P7 (1.84 ± 0.12 msec) to P13–P14 (0.64 ± 0.05 msec), as reported previously (Taschenberger and

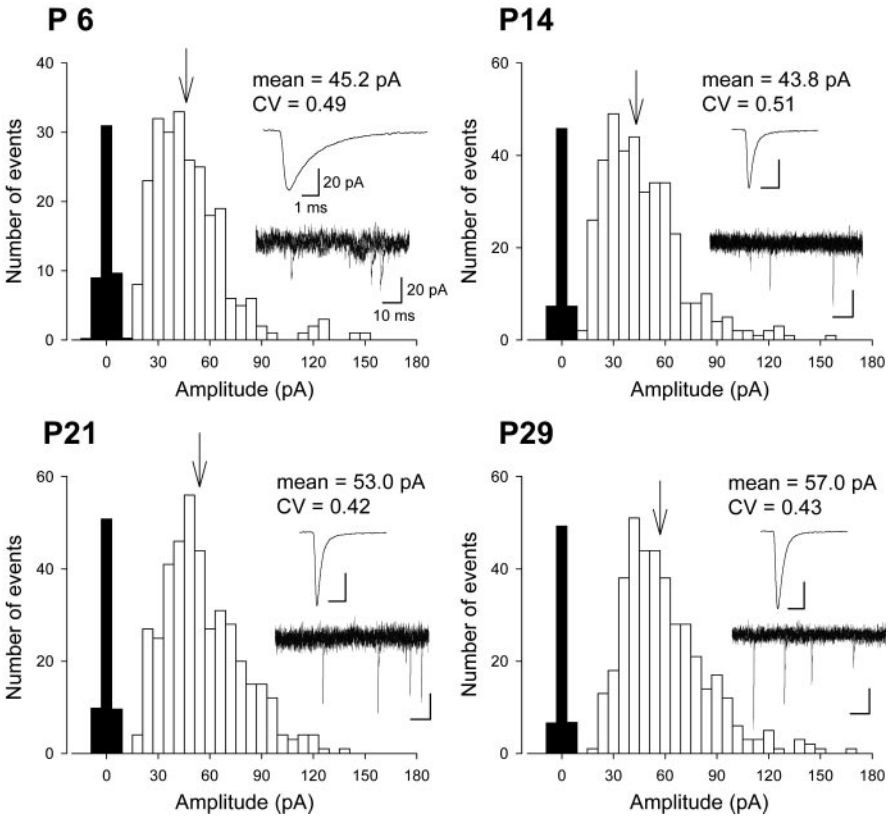

Figure 1. Miniature EPSCs recorded from MNTB principal neurons in developing rats. Representative amplitude distributions of mEPSCs in P6, P14, P21, and P29 rats (number of events, 242, 370, 408, and 392) are shown with sample records (insets) of averaged mEPSCs (from all events of each distribution) (top inset) and superimposed records (4 traces) (bottom inset). Background noise distributions (filled bars) were obtained from the baselines of records with no clear events. Arrows indicate mean amplitude of mEPSCs. CV, Coefficient of variation (SD/mean) for the mEPSC amplitude.

von Gersdorff, 2000; Futai et al., 2001; Joshi and Wang, 2002). It then continued to decrease from P13–P14 to P20–P21 (0.33 ± 0.01 msec; $p < 0.03$) (Fig. 2*D*) [but see Futai et al. (2001) for mice] and reached a minimum level at that time (0.36 ± 0.02 msec at P28–P29). The developmental shortening of the decay time may arise from changes in the subunit composition of AMPA receptors (Caicedo and Eybalin, 1999), resultant speeding in the desensitization kinetics (Wall et al., 2002), and/or a decrease in burst duration of underlying channels (Takahashi et al., 1992).

Single-channel conductance of postsynaptic receptor channels underlying mEPSCs

A developmental increase in quantal size might be a result of an increase in the underlying single-channel conductance of AMPA receptors. We examined this possibility by applying the nonstationary fluctuation analysis (Sigworth, 1980; Robinson et al., 1991; Traynelis et al., 1993) to mEPSCs. The variance during the decay phase of individual mEPSCs was plotted against their mean amplitude, and the weighted mean single-channel current was estimated from the initial slope of the peak-scaled mean-variance relationship (Fig. 3). Single-channel conductance was 21.5 ± 1.5 pS at P13–P14 ($n = 8$) as reported previously (20.4 pS) (Sahara and Takahashi, 2001), which was essentially the same as those in older (P28–P29; 19.4 ± 1.9 pS; $n = 7$) and younger (P6–P7; 20.6 ± 1.7 pS; $n = 7$) rats ($p > 0.6$; ANOVA).

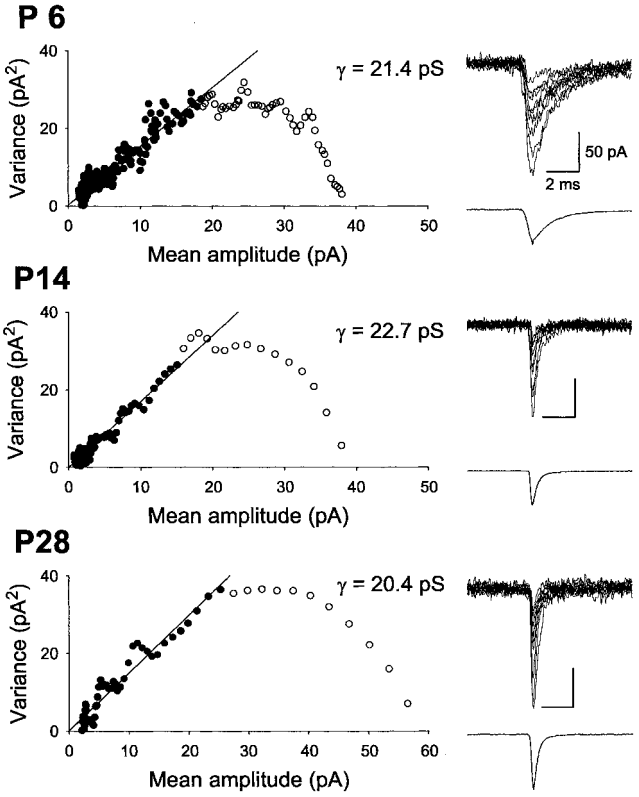

Figure 3. Single-channel conductance of AMPA receptors underlying mEPSCs. Right column, Individual mEPSCs (top) (10 records superimposed after peak alignment) and averaged mEPSCs (bottom) at P6, P14, and P28. Left column, Peak-scaled variance-mean current plots obtained by the nonstationary fluctuation analysis for mEPSCs in P6, P14, and P28 rats. These σ^2–I plots were calculated from 162, 341, and 371 events, respectively. Mean single-channel current was estimated from the initial slope of the σ^2–I relationships. To estimate single-channel conductance (γ), reversal potentials of mEPSCs were measured in each recording.

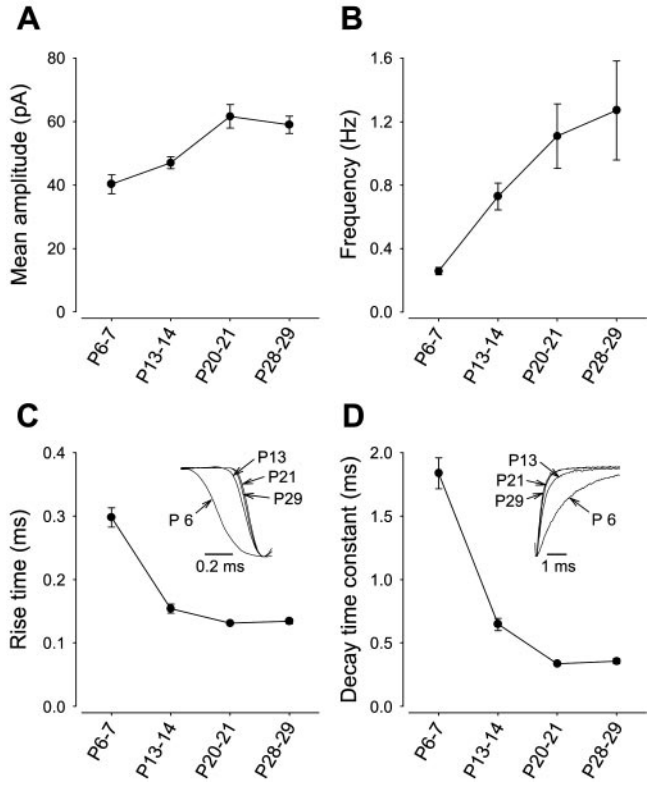

Figure 2. Developmental changes in the amplitude, frequency, and kinetics of mEPSCs. Miniature EPSCs were recorded from the MNTB principal neurons in rats at P6–P7, P13–P14, P20–P21, and P28–P29 ($n = 10$ for each). *A*, The mean amplitude of mEPSCs increased from P13–P14 to P20–P21. *B*, The mean frequency of mEPSCs increased from P6–P7 to P20–P21. *C*, The 10–90% rise time of mEPSCs decreased from P6–P7 to P13–P14. Sample records (inset) are the rising phases of average mEPSCs normalized at the peak. *D*, The weighted mean of decay time constants decreased significantly between P6–P7 and P13–P14 and between P13–P14 and P20–P21. Sample records (inset) are the decay phases of average mEPSCs normalized at the peak.

Developmental increase in the synaptic cleft concentration of transmitter liberated from each synaptic vesicle

Given that AMPA receptor channel conductance remains constant throughout development, a developmental increase in the mean quantal amplitude must arise from an increased number of receptors and/or increased concentration of transmitter in the synaptic cleft. Whereas the former possibility is technically difficult to assess, we examined the latter possibility by testing the effect of the rapidly dissociating AMPA receptor antagonist kynurenate on mEPSCs (Diamond and Jahr, 1997; Wadiche and Jahr, 2001). The inhibitory effect of kynurenate would be weaker if the glutamate concentration in the synaptic cleft is higher. As illustrated in Figure 4, kynurenate (50 μM) attenuated mEPSCs in both P13–P14 and P28–P29 rats, with the magnitude of inhibition at P28–P29 (20.8 ± 0.8%; $n = 7$) being significantly weaker than that at P13–P14 (26.9 ± 1.3%; $n = 7$; $p < 0.01$; Sheffe test) (Fig. 4*C*). To examine whether kynurenate can indeed detect changes in the glutamate concentration in the synaptic cleft, we loaded 50 mM L-glutamate into calyceal terminals at P13–P14 via presynaptic patch pipettes. The mean amplitude of mEPSCs recorded in this condition was larger than that of controls at P13–P14 but comparable with that of controls at P28–P29 (Fig. 4*B*) (Ishikawa et al., 2002). The inhibitory effect of kynurenate after presynaptic L-glutamate loading (17.8 ± 1.2%; $n = 5$) was signif-

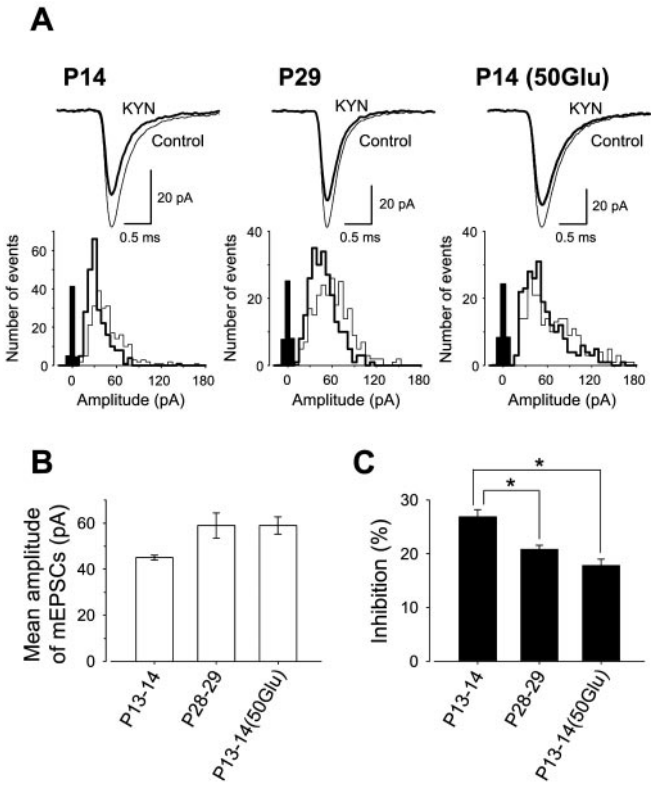

Figure 4. Developmental increase in the quantal transmitter concentration in the synaptic cleft detected by the low-affinity AMPA receptor antagonist kynurenate (KYN) (50 μM). *A*, Sample records (averaged from 243 events for each) and amplitude histograms of mEPSCs recorded from an MNTB neuron, before (thin line) and after (thick line) application of kynurenate (superimposed), each at P14, P29, and P14 with 50 mM L-glutamate (50Glu) loaded into a calyceal terminal. Filled bars are background noise histograms. *B*, *C*, Mean amplitude of mEPSCs (*B*) and their percentage inhibition by kynurenate (*C*) at P13–P14, P28–P29, and P13–P14 with 50 mM L-glutamate loaded into calyceal terminals. Asterisks indicate a significant difference with $p < 0.01$ (Sheffe test).

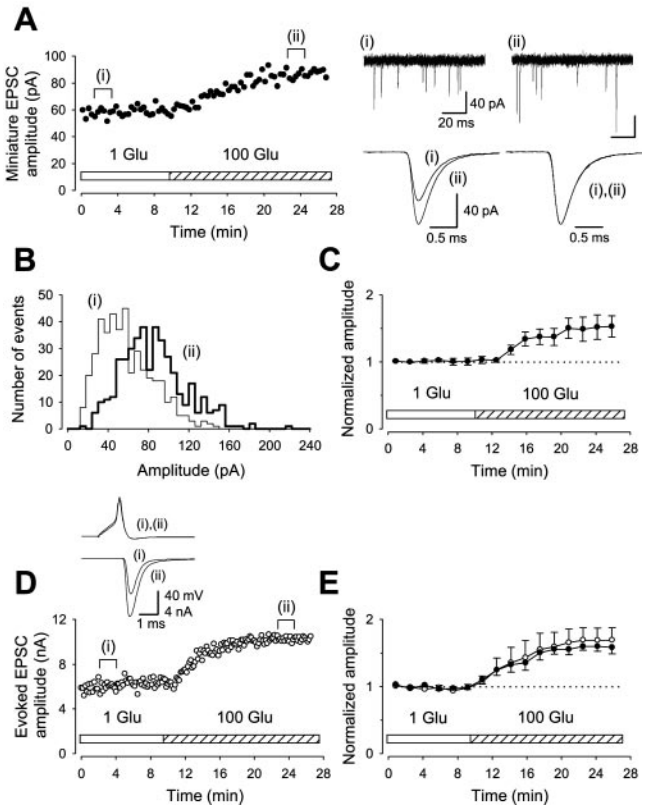

Figure 5. Nonsaturation of postsynaptic AMPA receptors at mature synapses. *A*, Miniature EPSCs recorded from a P28 MNTB neuron before (i) and after (ii) loading 100 mM L-glutamate into a calyceal terminal. Each data point represents the mean amplitude of mEPSCs sampled every 20 sec. Sample records of mEPSCs before (i) and after (ii) the L-glutamate loading at a slow sweep (top) and a fast sweep (bottom left, superimposed), and those normalized in the amplitude (bottom right, superimposed). *B*, Amplitude histograms of mEPSCs recorded from the same neuron before (i) and after (ii) the L-glutamate loading (number of events is 427 and 420, respectively). *C*, Summary data of mEPSCs from four synapses at P28–P29. The mean amplitude of mEPSCs before the L-glutamate loading was 54.3 ± 5.4 pA. *D*, Potentiation of evoked EPSCs by presynaptic loading of L-glutamate in a P29 rat. Sample records are averaged presynaptic action potentials (top, superimposed) and EPSCs before (i) and after (ii) the L-glutamate loading (bottom, superimposed). *E*, Summary data for evoked EPSCs (open circles) and spontaneous EPSCs (filled circles) from four synapses at P29. Before L-glutamate loading, the mean amplitude of evoked EPSCs was 4.37 ± 0.71 nA, and that of spontaneous EPSCs was 64.0 ± 10.6 pA. Glu, Glutamate. Dotted lines in *C* and *E* denote mean values of data points before L-glutamate loadings.

icantly weaker than controls at P13–P14 ($p < 0.01$) (Fig. 4*C*), confirming that kynurenate can reliably detect increased vesicular glutamate content. In contrast to kynurenate, the slowly dissociating AMPA receptor antagonist 2,3-dihydroxy-6-nitro-7-sulfonyl-benzo[*f*]quinoxaline (30 nM) attenuated mEPSCs in P13–P14 and P28–P29 rats to a similar extent, with the magnitude of inhibition being 31.1 ± 1.1% ($n = 5$) at P13–P14 and 31.6 ± 2.4% ($n = 4$) at P28–P29 ($p > 0.8$), indicating that the dissociation rate of antagonist must be fast to detect different glutamate concentrations in the synaptic cleft. These results also suggest that the affinity of AMPA receptor antagonists may not change much during development. Because the rise time of mEPSCs was unchanged from P13–P14 to P28–P29 (Fig. 2*C*), the diffusion distance from release sites to receptors seems unchanged. In fact, the morphological architecture of this synapse is established at P14 (Kandler and Friauf, 1993). Higher glutamate concentration in the synaptic cleft at mature synapses suggests that the amount of transmitter in each synaptic vesicle increases with development.

Nonsaturation of postsynaptic AMPA receptors

A quantal packet of transmitter does not saturate postsynaptic glutamate receptors at the calyx of Held synapse in P13–P15 rats (Ishikawa et al., 2002). Our results suggest that vesicular transmitter content increases with development after P13–P14. Therefore, the increased transmitter might then saturate postsynaptic AMPA receptors. We examined this possibility by loading a high concentration of L-glutamate directly into the calyceal nerve terminal via pipette perfusion in P28–P29 rats, while recording mEPSCs in the presence of TTX (Ishikawa et al., 2002). With 1 mM glutamate in the presynaptic pipette, amplitudes of mEPSCs were stable. After confirming a stable baseline, we infused 100 mM L-glutamate into the calyceal terminal via a perfusion pipette installed inside the patch pipette (Hori et al., 1999; Ishikawa et al., 2002). This caused a marked potentiation of mEPSCs ($p < 0.01$) (Fig. 5*A*), with their amplitude distribution clearly shifted toward larger events (Fig. 5*B*). No significant change was observed for the mean frequency of mEPSCs (99 ± 13%; $n = 4$). At four synapses, the mean magnitude of potentiation was 50 ± 12% (measured 13–15 min after glutamate infusion) (Fig. 5*C*). Despite the marked increase in the amplitude of mEPSCs, neither the rise time (10–90%; 0.13 ± 0.006 msec before and 0.13 ± 0.005 msec after switch; $n = 4$; $p > 0.9$) nor the decay time constant (0.32 ±

0.03 msec before and 0.32 ± 0.02 msec after switch; $n = 4$; $p > 0.8$) changed significantly (Fig. 5*A*). Unchanged rise time argues against the possibility that increased vesicular transmitter spilled over to remote receptors and increased the mEPSC amplitude (DiGregorio et al., 2002; Ishikawa et al., 2002). Whereas a positive correlation between rise time and amplitude of mEPSCs is taken as evidence for multiquantal release at other synapses (Paulsen and Heggelund, 1996; Wall and Usowicz, 1998), no such correlation was observed at this synapse, both before and after L-glutamate infusion ($r < 0.2$; $n = 4$ synapses). Also, the coefficient of variation of the mEPSC amplitude remained similar (91 ± 3%; $n = 4$; $p > 0.08$) after L-glutamate loading. These results argue against an involvement of multivesicular release in the potentiation of mEPSCs caused by presynaptic L-glutamate loadings. As expected from the results of mEPSCs, presynaptic loading of L-glutamate also potentiated EPSCs evoked by presynaptic action potentials at P29 (Fig. 5*D*), on average by 71 ± 16% ($n = 4$) (Fig. 5*E*). Spontaneous EPSCs recorded simultaneously with evoked EPSCs are equivalent to mEPSCs at this synapse, because TTX had no effect on the amplitude (102 ± 4%; $n = 4$) or frequency (104 ± 4%; $n = 4$) of spontaneous EPSCs in P29 rats compared with P13–P15 rats (Ishikawa et al., 2002). In addition to mEPSCs (Fig. 5*A–C*), spontaneous EPSCs underwent a clear potentiation (60 ± 6%; $n = 4$) (Fig. 5*E*). These results strongly suggest that quantal packets of transmitter do not saturate postsynaptic AMPA receptors even at the mature calyx of Held synapse.

Discussion

By making whole-cell recordings from presynaptic terminals and postsynaptic cells at the mature calyx of Held synapse, we have demonstrated that a quantal packet of transmitter does not saturate postsynaptic AMPA receptors. This implies that vesicular transmitter content can affect synaptic efficacy even in mature animals. Because vesicular glutamate is controlled by vesicular glutamate transporters (Burger et al., 1989) and indirectly via cytoplasmic glutamate concentration by glutamine and glial glutamate transporters (Danbolt, 2001), modulation of these transporters may influence synaptic efficacy at mature synapses as well as at immature synapses (Ishikawa et al., 2002).

The calyx of Held synapse is formed at approximately P5 and undergoes morphological transformations until P14, at which the adult-like calyceal structure is established (Kandler and Friauf, 1993). Rodents start to hear sounds during the second postnatal week (P10–P13) (Futai et al., 2001). During this critical week, the calyx of Held synapse undergoes various molecular and functional changes, such as downregulation of NMDA receptors (Futai et al., 2001; Joshi and Wang, 2002), switch of voltage-dependent Ca^{2+} channel subtypes (Iwasaki and Takahashi, 1998), a decrease in the transmitter release probability, and an increase in size of the readily releasable pool of synaptic vesicles (Taschenberger and von Gersdorff, 2000; Iwasaki and Takahashi, 2001). After P14, postsynaptic NMDA receptors continue to decrease toward P27, at which time the high-fidelity synaptic transmission is established (Futai et al., 2001). Our present results also demonstrate that the mean amplitude, mean frequency, and kinetics of mEPSCs reach steady levels at P20–P21, suggesting that the calyx of Held synapse becomes functionally mature at this period.

A developmental increase in mean quantal amplitude can be caused by an increase in vesicular transmitter content or in postsynaptic receptor density. Our results with kynurenate support the presence of the former mechanism but do not at all rule out the latter mechanism. Direct loading of a high concentration of L-glutamate into the calyces increased the quantal amplitude by 50% on average in P28–P29 rats, suggesting that the occupancy of postsynaptic AMPA receptors by a single quantum is still <67% as estimated at P13–P15 (<60%) (Ishikawa et al., 2002). It is possible that the postsynaptic density of AMPA receptors increases with development, thereby maintaining low receptor occupancy by quantal transmitter. Although quantal transmitter does not saturate NMDA receptors in P13–P15 rats (Ishikawa et al., 2002), it remains unknown whether it does so in mature animals with decreased NMDA receptor expression (Futai et al., 2001).

Developmental reduction in the basal release probability during the second postnatal week reduces synaptic depression, thereby increasing synaptic efficacy for high-frequency transmission (Taschenberger and von Gersdorff, 2000; Iwasaki and Takahashi, 2001). The developmental increase in the quantal amplitude observed in this study should increase the synaptic efficacy regardless of the frequency of transmission, thereby contributing to improving stability of high-fidelity transmission for sound localization at the calyx of Held synapse.

References

Burger PM, Mehl E, Cameron PL, Maycox PR, Baumert M, Lottspeich F, De Camilli P, Jahn R (1989) Synaptic vesicles immunoisolated from rat cerebral cortex contain high levels of glutamate. Neuron 3:715–720.

Caicedo A, Eybalin M (1999) Glutamate receptor phenotypes in the auditory brainstem and mid-brain of the developing rat. Eur J Neurosci 11:51–74.

Chuhma N, Ohmori H (1998) Postnatal development of phase-locked high-fidelity synaptic transmission in the medial nucleus of the trapezoid body of the rat. J Neurosci 18:512–520.

Clements JD, Lester RA, Tong G, Jahr CE, Westbrook GL (1992) The time course of glutamate in the synaptic cleft. Science 258:1498–1501.

Danbolt NC (2001) Glutamate uptake. Prog Neurobiol 65:1–105.

Diamond JS, Jahr CE (1997) Transporters buffer synaptically released glutamate on a submillisecond time scale. J Neurosci 17:4672–4687.

DiGregorio DA, Nusser Z, Silver RA (2002) Spillover of glutamate onto synaptic AMPA receptors enhances fast transmission at a cerebellar synapse. Neuron 35:521–533.

Evers J, Laser M, Sun YA, Xie ZP, Poo MM (1989) Studies of nerve-muscle interactions in *Xenopus* cell culture: analysis of early synaptic currents. J Neurosci 9:1523–1539.

Forsythe ID, Barnes-Davies M (1993) The binaural auditory pathway: membrane currents limiting multiple action potential generation in the rat medial nucleus of the trapezoid body. Proc R Soc Lond B Biol Sci 251:143–150.

Frerking M, Wilson M (1996) Saturation of postsynaptic receptors at central synapses? Curr Opin Neurobiol 6:395–403.

Futai K, Okada M, Matsuyama K, Takahashi T (2001) High-fidelity transmission acquired via a developmental decrease in NMDA receptor expression at an auditory synapse. J Neurosci 21:3342–3349.

Hori T, Takai Y, Takahashi T (1999) Presynaptic mechanism for phorbol ester-induced synaptic potentiation. J Neurosci 19:7262–7267.

Ishikawa T, Sahara Y, Takahashi T (2002) A single packet of transmitter does not saturate postsynaptic glutamate receptors. Neuron 34:613–621.

Iwasaki S, Takahashi T (1998) Developmental changes in calcium channel types mediating synaptic transmission in rat auditory brainstem. J Physiol (Lond) 509:419–423.

Iwasaki S, Takahashi T (2001) Developmental regulation of transmitter release at the calyx of Held in rat auditory brainstem. J Physiol (Lond) 534:861–871.

Jack JJ, Redman SJ, Wong K (1981) The components of synaptic potentials evoked in cat spinal motoneurones by impulses in single group Ia afferents. J Physiol (Lond) 321:65–96.

Jonas P, Major G, Sakmann B (1993) Quantal components of unitary EPSCs at the mossy fibre synapse on CA3 pyramidal cells of rat hippocampus. J Physiol (Lond) 472:615–663.

Joshi I, Wang LY (2002) Developmental profiles of glutamate receptors and synaptic transmission at a single synapse in the mouse auditory brainstem. J Physiol (Lond) 540:861–873.

Kandler K, Friauf E (1993) Pre- and postnatal development of efferent connections of the cochlear nucleus in the rat. J Comp Neurol 328:161–184.

Larkman A, Stratford K, Jack J (1991) Quantal analysis of excitatory synaptic action and depression in hippocampal slices. Nature 350:344–347.

Liu G, Choi S, Tsien RW (1999) Variability of neurotransmitter concentration and nonsaturation of postsynaptic AMPA receptors at synapses in hippocampal cultures and slices. Neuron 22:395–409.

Mainen ZF, Malinow R, Svoboda K (1999) Synaptic calcium transients in single spines indicate that NMDA receptors are not saturated. Nature 399:151–155.

McAllister AK, Stevens CF (2000) Nonsaturation of AMPA and NMDA receptors at hippocampal synapses. Proc Natl Acad Sci USA 97:6173–6178.

Okada M, Onodera K, Van Renterghem C, Sieghart W, Takahashi T (2000) Functional correlation of $GABA_A$ receptor α subunit expression with the properties of IPSCs in the developing thalamus. J Neurosci 20:2202–2208.

Paulsen O, Heggelund P (1996) Quantal properties of spontaneous EPSCs in neurons of the guinea-pig dorsal lateral geniculate nucleus. J Physiol (Lond) 496:759–772.

Robinson HP, Sahara Y, Kawai N (1991) Nonstationary fluctuation analysis and direct resolution of single channel currents at postsynaptic sites. Biophys J 59:295–304.

Sahara Y, Takahashi T (2001) Quantal components of the excitatory postsynaptic currents at a rat central auditory synapse. J Physiol (Lond) 536:189–197.

Sigworth FJ (1980) The variance of sodium current fluctuations at the node of Ranvier. J Physiol (Lond) 307:97–129.

Silver RA, Cull-Candy SG, Takahashi T (1996) Non-NMDA glutamate receptor occupancy and open probability at a rat cerebellar synapse with single and multiple release sites. J Physiol (Lond) 494:231–250.

Singer JH, Talley EM, Bayliss DA, Berger AJ (1998) Development of glycinergic synaptic transmission to rat brain stem motoneurons. J Neurophysiol 80:2608–2620.

Song HJ, Ming GL, Fon E, Bellocchio E, Edwards RH, Poo MM (1997) Expression of a putative vesicular acetylcholine transporter facilitates quantal transmitter packaging. Neuron 18:815–826.

Takahashi T, Momiyama A, Hirai K, Hishinuma F, Akagi H (1992) Functional correlation of fetal and adult forms of glycine receptors with developmental changes in inhibitory synaptic receptor channels. Neuron 9:1155–1161.

Takahashi T, Forsythe ID, Tsujimoto T, Barnes-Davies M, Onodera K (1996) Presynaptic calcium current modulation by a metabotropic glutamate receptor. Science 274:594–597.

Tang CM, Margulis M, Shi QY, Fielding A (1994) Saturation of postsynaptic glutamate receptors after quantal release of transmitter. Neuron 13:1385–1393.

Taschenberger H, von Gersdorff H (2000) Fine-tuning an auditory synapse for speed and fidelity: developmental changes in presynaptic waveform, EPSC kinetics, and synaptic plasticity. J Neurosci 20:9162–9173.

Tong G, Jahr CE (1994) Multivesicular release from excitatory synapses of cultured hippocampal neurons. Neuron 12:51–59.

Traynelis SF, Silver RA, Cull-Candy SG (1993) Estimated conductance of glutamate receptor channels activated during EPSCs at the cerebellar mossy fiber-granule cell synapse. Neuron 11:279–289.

Umemiya M, Senda M, Murphy TH (1999) Behaviour of NMDA and AMPA receptor-mediated miniature EPSCs at rat cortical neuron synapses identified by calcium imaging. J Physiol (Lond) 521:113–122.

Wadiche JI, Jahr CE (2001) Multivesicular release at climbing fiber-Purkinje cell synapses. Neuron 32:301–313.

Wall MJ, Usowicz MM (1998) Development of the quantal properties of evoked and spontaneous synaptic currents at a brain synapse. Nat Neurosci 1:675–682.

Wall MJ, Robert A, Howe JR, Usowicz MM (2002) The speeding of EPSC kinetics during maturation of a central synapse. Eur J Neurosci 15:785–797.